frontiers | Frontiers in Materials

TYPE Original Research
PUBLISHED 20 October 2022
DOI 10.3389/fmats.2022.1050074

OPEN ACCESS

EDITED BY
Lik-Ho Tam,
Beihang University, China

REVIEWED BY
Muhammad Khan,
University of Warwick, United Kingdom
Puhui Chen,
Nanjing University of Aeronautics and Astronautics, China
Alexander Protsenko,
Komsomolsk-na-Amure State University, Russia

*CORRESPONDENCE
Yang Zhang,
composite123@sina.com

SPECIALTY SECTION
This article was submitted to Polymeric and Composite Materials, a section of the journal Frontiers in Materials

RECEIVED 21 September 2022
ACCEPTED 10 October 2022
PUBLISHED 20 October 2022

CITATION
Wang F, Zhang YC, Hu S and Zhang Y (2022), Preparation and curing process optimization of an asymmetric impregnated vacuum bag-only prepreg. *Front. Mater.* 9:1050074.
doi: 10.3389/fmats.2022.1050074

Preparation and curing process optimization of an asymmetric impregnated vacuum bag-only prepreg

Feng Wang, Yi Chuan Zhang, Su Hu and Yang Zhang*

AVIC Composite Corporation LTD, Beijing, China

One of the most significant defects, porosity, has been proven to affect the properties of composites. It is critical to reduce the porosity of composite material and the curing cost while maintaining high laminate quality for vacuum bag-only prepreg. In this paper, a rapidly cured epoxy resin system was developed, and an alkali-free glass fiber fabric prepreg suitable for vacuum bag molding was prepared by the asymmetric impregnation method. The optimal curing process for the prepreg was determined by resin curing kinetics, dielectric viscosity, initial curing temperature, and curing time of the prepreg on the laminate quality. The optimal curing profile of the prepreg was obtained. In addition, the effect of room temperature exposure time on the properties of the prepreg was also evaluated. These laminates produced by vacuum bag molding had outstanding internal quality and mechanical properties *via* the changes in the asymmetric impregnation process and the curing procedure.

KEYWORDS

vacuum bag-only, asymmetric impregnation, porosity, curing process optimization, mechanical properties

Introduction

Resin-based composite materials are widely used in aerospace applications since their lightweight, high strength, strong designability, corrosion resistance, and excellent fatigue resistance (Mooney, 1991; Panettieri et al., 2016; Wang et al., 2022). The application range of advanced resin-based composite materials in the aerospace field has gradually been applied from secondary load-bearing structures such as fairings and rudder surface structures to large-scale primary load-bearing structures such as aircraft wings and fuselage panels (Orifici et al., 2008). In addition, autoclave molding is the primary process for large composite structures (Abdelal et al., 2013; Lionetto et al., 2017). The composite components produced by autoclave molding include the advantages of high mechanical properties, low porosity, and good quality stability. However, the manufacturing costs are exorbitant. The resin-based composite materials can also be heated and cured in a curing furnace (oven) by vacuum bag molding (Hou et al., 2013; Centea et al., 2015; Dong et al., 2018; Schechter et al., 2018). Usually, the curing cost of the

oven is 10%~20% of the cost of an autoclave of the same size (Centea et al., 2015). As resin composites' applications become increasingly extensive, the demand for low-cost composite systems and their molding processes becomes urgent.

Porosity, an essential factor, influences the mechanical properties of composite materials (Costa et al., 2001; Hernández et al., 2011; Agius et al., 2013; Torres et al., 2018). Aerospace structural composites require a porosity of less than 1% for the primary load-bearing structure and less than 2% for the secondary load-bearing structure. When the traditional autoclave curing prepreg adopts the vacuum bag molding process, the porosity of the composite materials will generally exceed 2%. Moreover, the vacuum pressure can only be applied in the vacuum bag-only prepreg curing process. To control the porosity of the part and make the composite materials reach the same mechanical performance index as autoclave molding, the structural form of the prepreg (Hou et al., 2013), the performance of the resin matrix (Marycheva, 2014), and the curing process of the prepreg must be changed (Carbas et al., 2014; Takagaki et al., 2016).

Typically, VBO prepreg is accomplished by partially impregnated fibers, thereby creating incompletely impregnated dry fiber pathways in the prepreg (Uthemann et al., 2017; Pang et al., 2021). The dry fiber layer provides an engineering vacuum air channel (EVAC) for gases and volatiles, which can effectively reduce composite porosity. In the vacuum bag molding process, it is crucial to choose the appropriate temperature by balancing the resin flow time (Hubert and Poursartip, 1998; Li et al., 2007) and gel time (Martínez-Miranda et al., 2019) for the initial curing so that the resin impregnates the dry fiber layer and discharges volatiles before gelation (Liu et al., 2011; Zhou et al., 2014). If the initial curing temperature is high, the resin will be well impregnated, and the gas channel will be blocked before the volatiles is discharged. Meanwhile, the higher temperature may also cause the resin to cross-link quickly and increase the resin viscosity. The excessively high temperature will hinder the removal of interlayer gases and volatiles and eventually lead to the excessively high porosity of the composites. Conversely, suppose the initial curing temperature is too low, the impregnability of the resin will be poor, producing dry fibers that are not sufficiently impregnated and resulting in high compositional porosity.

To take advantage of the vacuum bag molding process, reducing production costs while maintaining the high quality of the laminate, the team independently developed a medium-temperature curing epoxy suitable for vacuum bag molding. Based on this resin system, an asymmetrically impregnated alkali-free glass fiber fabric prepreg with controllable impregnation was successfully fabricated *via* a two-step hot-melt process. In addition, the vacuum bag molding procedures were optimized by evaluating resin curing thermodynamics, initial curing temperature, and curing time on the final laminate quality. These factors also helped determine the prepreg curing process curve. Furthermore, the optimization included evaluating room temperature exposure time on the properties of the composites.

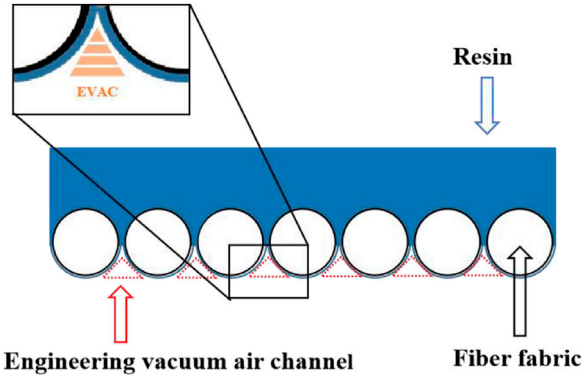

FIGURE 1
Schematic diagram of asymmetric impregnation of the prepreg.

Materials and methods

Materials

The developed epoxy resin system with vacuum bag molding was used in the study, which contained a multifunctional epoxy novolac and a thermoplastic polyurethane. This system used dicyandiamide as a curing agent and methylene diphenyl dimethyl urea as a curing accelerator. The epoxy value was 0.5. The percentage of thermoplastic modifiers in the resin was 15%. The mass ratio of epoxy resin to dicyandiamide and curing accelerator was 100:1.5:1. The alkali-free glass fiber fabric EW301 F was purchased from Nanjing Glass Fiber Research Institute. Prepregs based on resin impregnated with E-glass fiber fabrics were prepared by a conventional hot melt two-step method (Wang et al., 2011). The resin content of the prepreg was 38%, and the fiber area weight was 295 g/m^2. The prepreg was prepared by single-sided asymmetric infiltration, and the degree of impregnation was 40~60%, controlling the corresponding process parameters (Figure 1). The EVAC is the unimpregnated dry fiber area, providing exhaust pathways for gases and volatiles.

Thermodynamic analysis

Non-isothermal thermodynamic measurements were conducted with a NETZSCH 200F3 differential scanning calorimeter (Germany). The samples were heated from 25°C to 250°C, and the heating rates were 5°C/min, 10°C/min, 15°C/

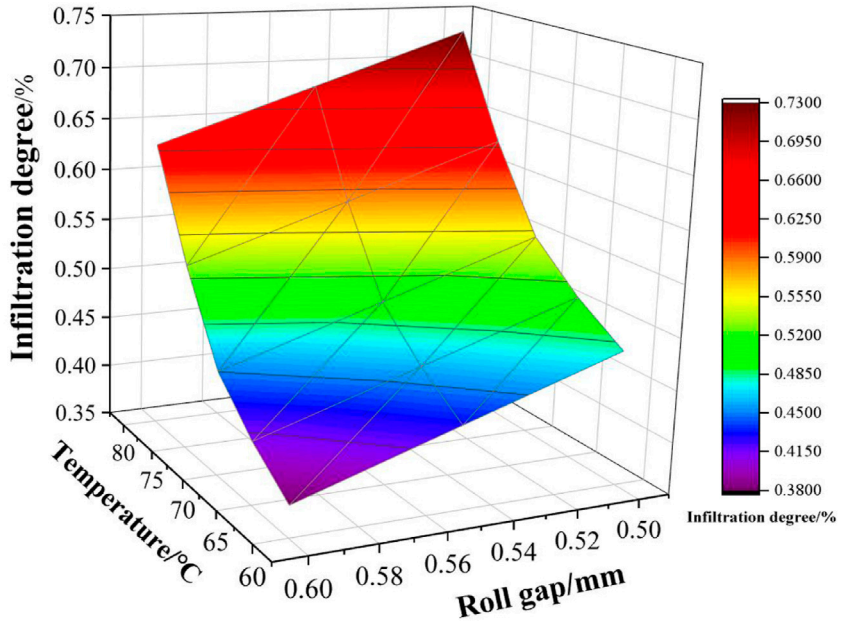

FIGURE 2
The relationship between the roll gap, the impregnation temperature and fiber fabric infiltration degree.

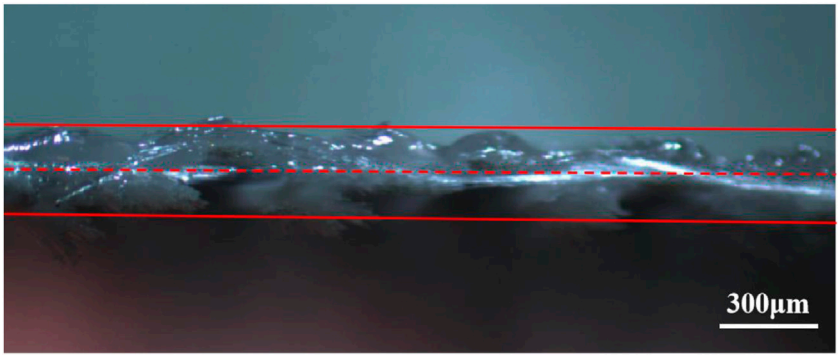

FIGURE 3
Optical micrograph of fiber fabric impregnation degree.

min, and 20°C/min, respectively. The weight of each sample was (7~10) mg. All DSC measurements were conducted in nitrogen atmosphere with a flow rate of 50 ml/min.

Viscosity

Resin viscosity measurements were conducted with a TA AR 2000ex rheometer (USA) using 25 mm diameter parallel plates with the frequency of 10 rad/s. In each test, the clamp gap was set to 1mm, and the stress was set to 10 Pa to study the effect of different temperatures on the resin viscosity. The resin samples were used around 1.5 g and heated from 25°C to 70°C, 80°C and 90°C, respectively, at a heating rate of 2°C/min and then kept for 60 min.

Ion viscosity

Ion viscosity measurements were conducted on a NETZSCH DEA288 dielectric resin curing instrument (Germany). The interdigitated electrode (IDEX-electrode Spacing 115 μm) sensor

TABLE 1 Resin system kinetic parameters.

β/K· min^{-1}	T_p^{-1}/K^{-1}	E_α (KJ·mol^{-1})	A	n
5	2.463 × 10^{-3}		7.713×10^{10}	
10	2.410 × 10^{-3}		8.364×10^{10}	
15	2.371 × 10^{-3}	88420.04	7.982×10^{10}	0.8923
20	2.343 × 10^{-3}		7.736×10^{10}	
Average	-		7.949×10^{10}	

β—heating rate, K/min; T_p—peak temperature, K; E_α—apparent activation energy, KJ/mol; R—ideal gas constant, 8.314 J/(mol·K); n-reaction orders; A-pre-exponential factor.

was used with a frequency of 10 Hz. The resin was heated from 30°C to 80°C for 40 min, and then heated to 127°C for 240 min at a heating rate of 2°C/min.

Glass transition temperature

Glass transition temperature measurements were conducted on a TA Q800 DMA instrument (USA) at a frequency of 1 Hz. The testing mode was three-point bending. The dimension of samples was 30 mm × 6 mm × 2 mm. The test temperature range was 30~180°C. The temperature rate was 5°C/min.

TABLE 2 T_i, T_p, and T_f Calculated with Different β.

β/°C·min^{-1}	T_i/°C	T_p/°C	T_f/°C
5	115.9	132.8	158.4
10	124.6	141.8	178.0
15	130.3	148.7	187.9
20	134.4	153.7	199.2

Porosity

The density of the resin, the reinforcement, and the composites were measured separately on a Mettler Toledo ME 204 analytical balance (USA) with ASTM D792 standard test method. Then composites void content was calculated by ASTM D2734 standard test method.

Ultrasound C-scan

The composite material laminate was inspected internally using the CUS-6000 large-scale ultrasonic automatic scanning imaging inspection equipment of AVIC Composite Corporation LTD. (China).

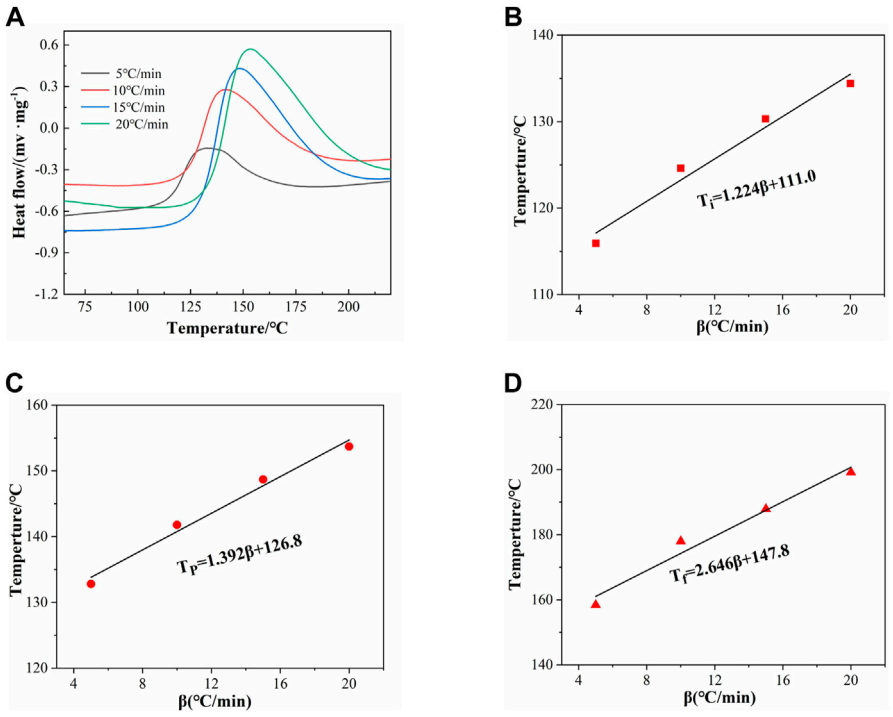

FIGURE 4
Resin curing kinetic parameters **(A)** DSC curves of VBO resin system; **(B)** The extrapolation plot of β-T_i; **(C)** The extrapolation plot of β-T_p; **(D)** The extrapolation plot of β-T_f.

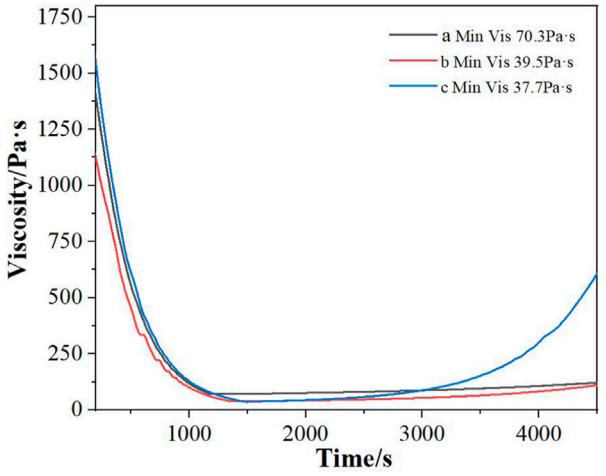

FIGURE 5
The relationship between viscosity and initial curing temperature of VBO resin system (a) at 70°C; (b) at 80°C; (c) at 90°C.

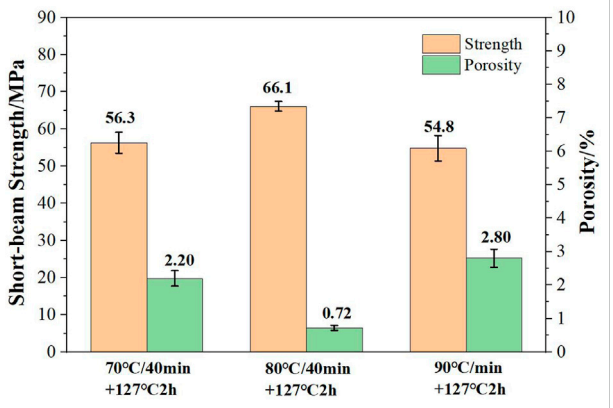

FIGURE 6
Effect of initial curing temperature on mechanical properties and void content of laminates.

Microstructure

The fracture surfaces of samples were examined *via* a FEI Quanta FEG 250 (USA) scanning electron microscope. The fracture surfaces were sputter-coated with gold before taking the micrographs. The section microstructure was studied by a Caikon XTL-3400C optical microscope (China).

Mechanical properties

The mechanical properties were tested on an Instron 5967 instrument (USA). The test standards for tensile and short beam shear tests were ASTM D3039 and ASTM D2344, respectively. At least five parallel samples were measured for each component and averaged.

Results

Preparation of asymmetric impregnated prepreg

The traditional preparation process produces autoclave prepreg in a sandwich structure, including a layer of reinforcing fiber fabric sandwiched between the upper and lower layers of resin films. The resin is thoroughly impregnated with the reinforcing fabric as a whole. The VBO prepreg optimized in this paper was adopted to the single-sided film impregnation technology, which focused on adjusting the two main process parameters related to the infiltration degree percentage. Two parameters are the roll gap and the impregnation temperature (Figure 2). The corresponding parameters were set to prepare the asymmetrically infiltrated prepreg according to the combination of the relevant curing process. Also, the optical microscope photo shows the fiber fabric's impregnation state, and the impregnation degree of the fiber fabric was between 40% and 60% (Figure 3).

Resin curing kinetic parameters

The study of resin curing kinetic parameters has theoretical significance for resin application (Chen et al., 2008; Moreau, 2021; Zhu et al., 2021; Cruz-Cruz et al., 2022). The curing kinetic equations involve a variety of parameters that have important implications for understanding the curing reaction, such as the apparent activation energy (E_α) and the reaction energy level (n). The value of E_α reflects the ease of curing system, while the complexity of curing a system is usually assessed by the number of reaction orders (n). The data were obtained using the Kissinger and Ozawa equation (Eqs 1–7), which involves processing the DSC data at different ramp rates (Ding et al., 2017; Liu et al., 2020). A linear fitting method was then processed to determine the kinetic parameters of the resin. Finally, the *n*th order kinetic model equation for curing the resin system was determined.

$$\frac{d\alpha}{dt} = K(T)(1-\alpha)^n \tag{1}$$

$$\ln\left(\frac{\beta}{T_P^2}\right) = \ln\left(\frac{AR}{E_\alpha}\right) - \left(\frac{E_\alpha}{RT_P}\right) \tag{2}$$

$$A = \left[\beta E_\alpha \exp\left(E_\alpha/RT_P\right)\right]/RT_P^2 \tag{3}$$

$$\frac{d\ln\beta}{d(1/T_P)} = -\left(E_\alpha/nR + 2T_P\right) \tag{4}$$

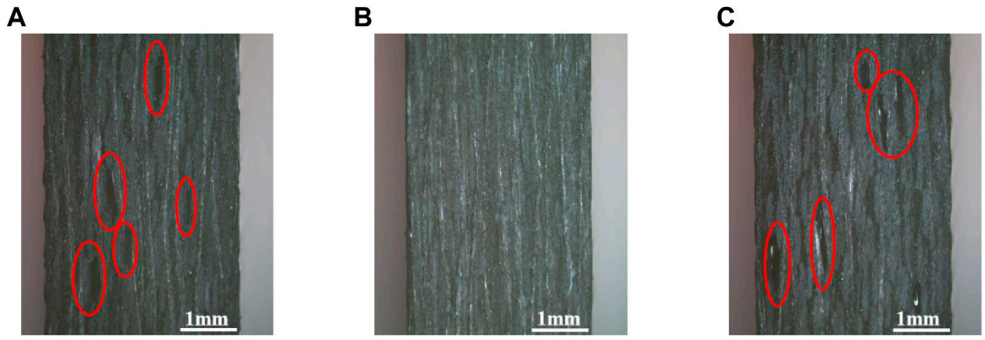

FIGURE 7
Optical micrograph of laminates cured at different initial curing temperature **(A)**70°C/40 min + 127°C/2 h; **(B)** 80°C/40 min + 127°C/2 h; **(C)** 90°C/40 min + 127°C/2 h.

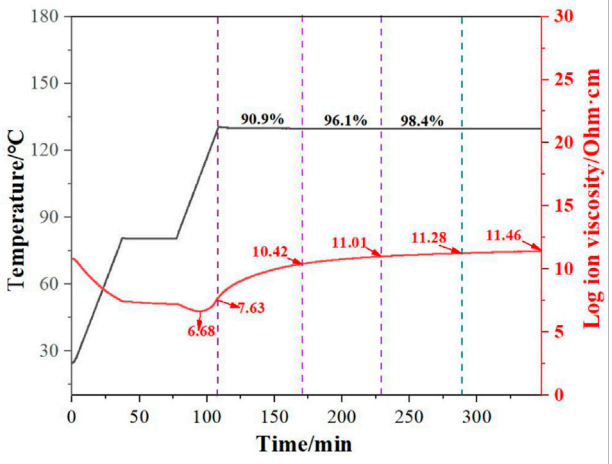

FIGURE 8
The relationship between the dielectric viscosity and the curing process curve of VBO resin system.

$$\frac{d\ln\beta}{d(1/T_P)} = -\frac{E_\alpha}{nR} \quad (5)$$

$$K = A\,exp(-E_\alpha/RT_P) \quad (6)$$

$$\frac{d(\alpha)}{d(t)} = A\,exp(-E_\alpha/RT)(1-\alpha)^n \quad (7)$$

Resin system kinetic parameters are shown in Table 1. The calculated A, E_α, n into the Eq. 7, to obtain the curing reaction kinetic equation $d\alpha/dt = 7.949 \times 10^{10} \exp(-10635.80/T)(1-\alpha)^{0.8923}$ (Ferdosiana et al., 2015; Leena et al., 2017). n = 0.8923, indicating that the resin reaction process is complex, but there is no multistage reaction. From the equation, the curing reaction rate is proportional to the reaction temperature, and the degree of cure is inversely related.

As the heating rate increases, the curing reaction's initial temperature and the maximum exothermic peak move toward the higher temperature in the resin system (Figure 4A; Table 2). The variation of temperature (T) and heating rate (β) conforms to the formula T = A+ Bβ. The temperature with the heating rate of 0°C/min extrapolated by T-β equation was used as the reliable curing temperature of the resin system. The linear fitting relationships of peak initial temperature (gelation temperature, T_i), peak temperature (Curing temperature, T_p), and peak-end temperature (post curing temperature, T_f) were obtained, respectively (Figures 4B,C,D). Based on the T-β extrapolation method, the necessary theoretical basis for the curing process of the composite material system was provided. The results showed that T_i was 110.0°C, T_p was 126.8°C, and T_f was 147.8°C.

Initial curing temperature optimization

Discharging as much as possible gases and volatiles before the resin gelation helps reduce the porosity of the composite materials for vacuum bag molding. Setting an initial curing temperature lower than the gel temperature is necessary for the discharging. Various initial curing temperatures were applied to cure the developed VBO prepreg stack, and the effect of the initial curing temperature was evaluated for the suitable cure cycle. The stacking sequence of $[0]_{12}$ was selected for all laminates. The VBO resin system was heated from room temperature to the initial curing temperature at a heating rate of 2°C/min for 40 min in the initial curing stage (Figure 5). And then, all laminates were heated to 127°C at the same heating rate (2°C/min) for 2 h.

After finishing the curing process, the laminates were analyzed with short-beam shear strength, porosity, and microstructures (Figures 6, 7). When the initial curing temperature was at 70°C and the minimum viscosity of the resin was 70.3 Pas, the apparent interlayer voids could be observed in the final composite materials with porosity of 2.2% and short beam strength of 56.3 MPa. At 70°C, the

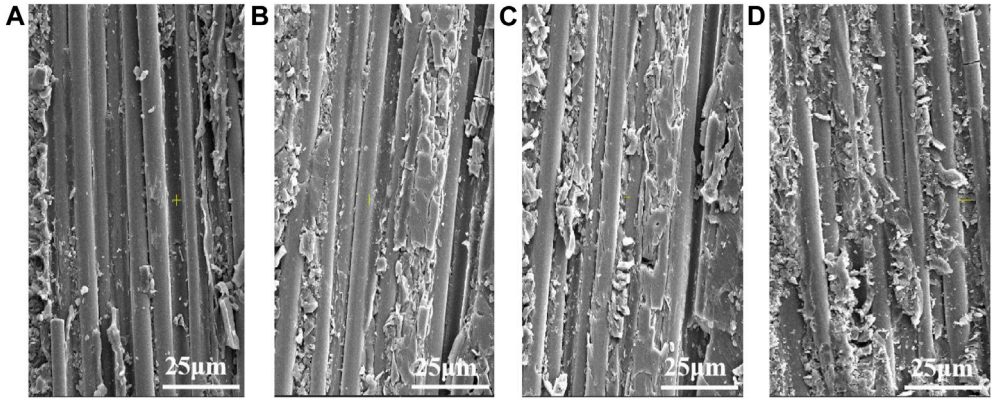

FIGURE 9
The SEM images of fracture surface in short-beam shear tests of laminates cured at 127°C for various time **(A)** for 1 h; **(B)** for 2 h; **(C)**for 3 h; **(D)** for 4 h.

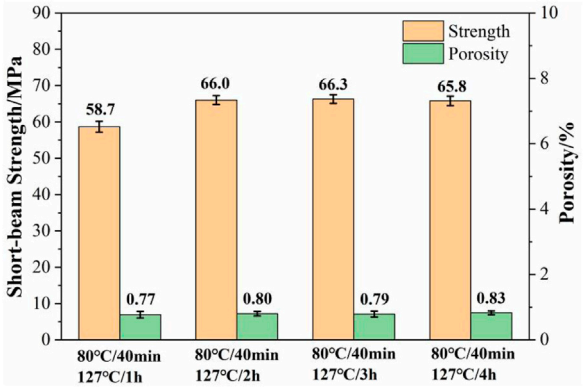

FIGURE 10
The effect of curing time on mechanical properties and void content of laminates.

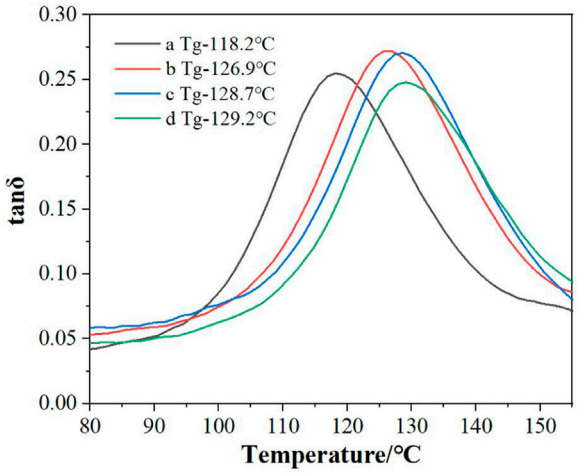

FIGURE 11
The effect of curing time on glass transition temperature (a) 80°C/40min +127°C/1 h; (b) 80°C/40min +127°C/2 h; (c) 80°C/40min +127°C/3 h; (d) 80°C/40min +127°C/4 h.

developed resin had high viscosity and poor flowability, and the resin was unable to penetrate each prepreg layer, resulting in the formation of final voids. On the contrary, the minimum viscosity of the resin was 37.7 Pas at 90°C, and the resin viscosity increased significantly in the holding stage, which hindered the resin impregnation process. The laminate porosity could be observed on the micrograph, with a porosity of 2.8% and short beam strength of 54.8 MPa for the composites. When the initial curing temperature of the composite materials was 80°C, the resin viscosity was 39.5 Pas, and the resin viscosity was stable in the initial curing stage. Meanwhile, the resin would complete infiltration after the gases between the prepreg layers were discharged entirely. Therefore, the laminate initially cured at 80°C had a maximum short beam shear strength of 66.1 MPa and a minimum porosity of 0.72%, which proved that 80°C is suitable for the initial curing temperature for the developed resin.

Effect of curing time

Reducing the dwelling time in the process is beneficial to maintaining an excellent laminate quality with low manufacturing cost. Compared to traditional rheological testing (Mortimer et al., 2001), dielectric analysis involves tracking the curing progress of a

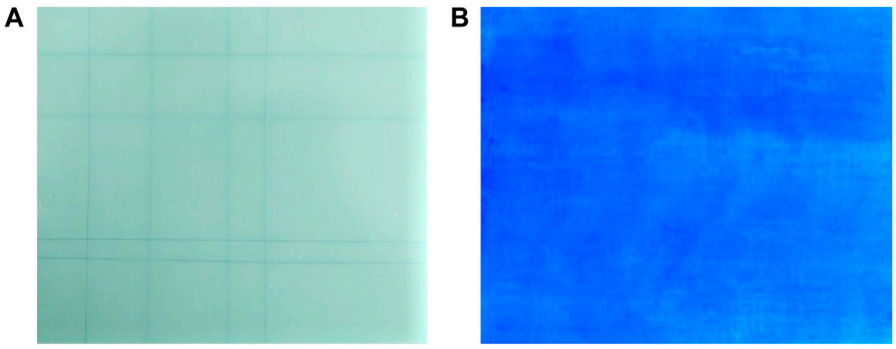

FIGURE 12
(A) Image of composite laminate; **(B)** C-scan image of non-destructive testing of composite laminate.

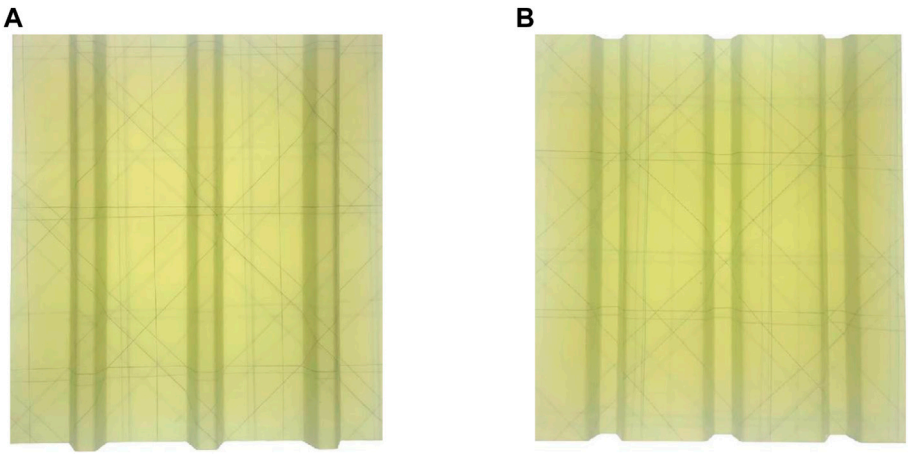

FIGURE 13
The translucent visual inspection of typical hat-shaped rib structure with the stacking sequence of $[+45/0/-45/90]_{2s}$ (400 mm × 500 mm × 4.24 mm) **(A)** front; **(B)** back.

resin and monitoring the change in resin's ionic resistivity (Pethrick and Hayward, 2002; Skordos and Partridge, 2004; Kim et al., 2014). The complete process from heating to curing can be characterized by dielectric viscosity (Figure 8) and made up for the lack of characterization of traditional rheological tests in the curing stage, guiding the composite materials' curing process. In the initial curing stage, the dielectric viscosity of the resin remained stable at 80°C, which indicated the resin did not undergo obvious cross-linking and curing, and the system was conducive to the discharge of volatiles. At 127°C, the cure degree of the resin for 1 h, 2 h, and 3 h curing time were 90.9%, 96.1%, and 98.4%, respectively. The improvement in the curing degree was not apparent when the curing time exceeded 2 h.

After optimized procedures were confirmed and characterized, the fracture surfaces of the laminates were analyzed *via* the short beam shear test, and the results were shown in SEM images (Figure 9). In the differential laminates' cured period (2, 3, and 4 h), a large amount of resin remained on the fibers' surfaces was observed on the fractured surfaces, which presented the fibers were strongly bonded to the resin matrix interface. When the laminate cured period was 1 h, it would result in a relatively low degree of resin curing. Since the bonding between resin and fiber matrix was relatively weak, and the fiber surface of the cross-section was smooth, there were fewer resin sticks.

All composites are cured and evaluated with short beam shear strength, porosity, and glass transition temperature by DMA, shown in Figures 10, 11. The highest porosity was less than 1.0% after the initial curing stage. The short beam shear

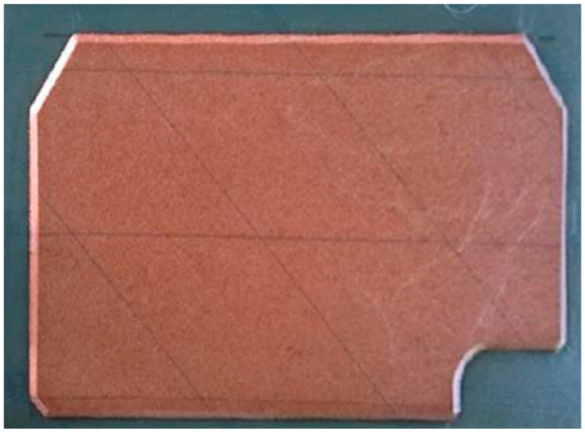

FIGURE 14
The typical sandwich structure of prepreg/PMI foam.

strength and glass transition temperature increased by 14% and 7.3%, respectively, after being cured for 2 h at 127°C, compared to the laminates cured for 1 h. However, as the curing period increased to three or 4 h, the short beam strength of the laminates improved slowly compared to 2 h, and the same conclusion was drawn for the glass transition temperature. Thus, the optimum curing time at 127°C was 2 h, which reached the balance between laminate quality improvement and manufacturing cost savings.

Preparation of typical structures of composite materials

Based on the optimized curing curve, the composite laminate (in the size of 220 mm × 240 mm × 6.33 mm) with the stacking sequence of $[0/90]_{6s}$ is obtained (Figure 12A). As a result, the laminate has excellent surface quality and a smooth appearance. Furthermore, the ultrasonic C-scan of the laminate presents the composite laminate in exquisite internal quality (Figure 12B). Compared with traditional ultrasonic nondestructive testing, translucent visual inspection significantly improves inspection efficiency and reduces inspection costs. As the developed composite materials can transmit light with a light source, the semi-transparent visual inspection of the composite material parts can be carried out utilizing optical aids (Meola, 2020). The translucent visual inspection photo of the hat-shaped rib structure proves an exquisite internal quality of the corrugated beam without defects such as inclusions and pores (Figure 13).

On the other hand, the prepreg/PMI foam, prepared by vacuum bag molding with the optimized curing process, reaches the quality requirements and has better quality than the traditional VBO prepreg in a sandwich structure, including the phenomenon of pores or poor glue (Figure 14). Furthermore, it confirms that the optimized curing process procedure for the VBO prepreg has strong applicability, not only for manufacturing large-thickness and complex structural laminates but also for preparing sandwich structures.

Mechanical properties of composite materials

The intuitive reflection of the developed composites by comparing the mechanical properties to Toray 7781/#2510 composites (Figure 15), in which resin and prepregs have been widely used in the general bearing structure of available aviation aircraft. In the curing process of Toray 7781/#2510, the initial curing temperature is 88°C for 90 min and 132°C for 120 min, which requires a higher temperature and longer curing time. The comparison includes composites cured in different exposure times. VBO-0d is the composites cured the same day after the prepreg preparation, and VBO-30d is the composites exposed for 30 days before curing. The performance of the optimized composite materials, produced

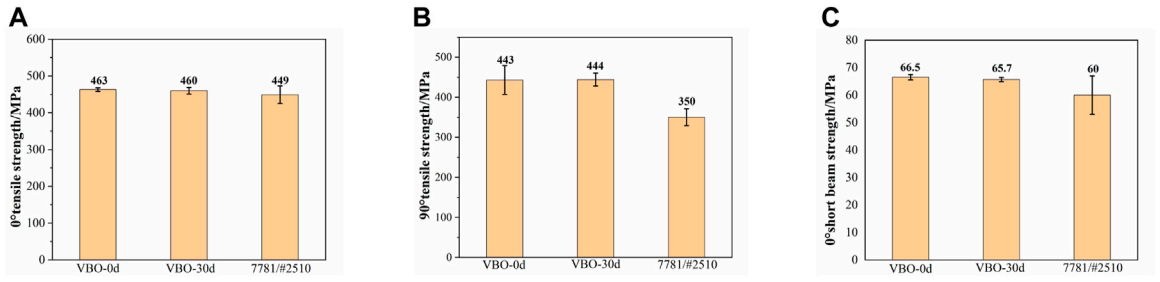

FIGURE 15
The comparison of the optimized composites and Toray's 7781/#2510 composites' vacuum bag molding mechanical properties **(A)** 0°tensile properties; **(B)** 90°tensile properties; **(C)** 0°short beam properties.

via vacuum bag molding, remains the same after exposure to room temperature for 30 days. Both composites present similar 0°tensile strength properties to Toray 7781/#2510 composites, with a 25.5% increase in 90°tensile strength and a 10% increase in short beam strength, concluding that the optimized prepreg has more potential applications in the civil aviation field.

Conclusion

In this research, a rapidly cured VBO resin has been independently developed. The asymmetrically impregnated VBO prepregs were fabricated *via* a more conventional two-step process. The theoretical gel temperature and curing temperature of the resin system were calculated by the T-β extrapolation method, and the effects of initial curing temperature and curing time on the final laminate quality were evaluated. When the initial curing temperature was 80°C, the resin viscosity was moderately enough for resin infiltration before gelation in the initial curing stage. Laminates had similar interlaminar strengths and glass transition temperatures with distinctive curing times (2, 3, and 4 h) in the curing stage at 127°C. However, the laminates cured for 1 h showed weaker interlaminar strength and lower glass transition temperature. The same results were also confirmed by the dielectric viscosity test and SEM fracture photographs. Based on that, an optimized rapidly cured program was determined with the curing time of 40 min at the initial curing temperature (80°C), followed by the curing temperature at 127°C for 2 h. The laminates cured with the optimized prepreg have excellent mechanical strength and transparency, which can be non-destructively inspected by the low-cost translucent visual inspection method. It is believed that the developed VBO prepreg is a favorable competitor for future general aviation industry applications.

Data availability statement

The raw data supporting the conclusion of this article will be made available by the authors, without undue reservation.

Author contributions

FW—formal analysis and writing manuscript, YCZ—investigating in the project, SH—reviewing and editing manuscript, YZ—conceptualization and methodology, project coordinator. All authors have read and agreed to the published version of the manuscript.

Funding

This research was funded by the major science and technology research and development project of Shunyi District, Beijing. (GZ292120301).

Conflict of interest

FW, YCZ, SH, and YZ were employed by the company AVIC Composite Corporation LTD.

Publisher's note

All claims expressed in this article are solely those of the authors and do not necessarily represent those of their affiliated organizations, or those of the publisher, the editors and the reviewers. Any product that may be evaluated in this article, or claim that may be made by its manufacturer, is not guaranteed or endorsed by the publisher.

References

Abdelal, G. F., Robotham, A., and Cantwell, W. (2013). Autoclave cure simulation of composite structures applying implicit and explicit FE techniques. *Int. J. Mech. Mater. Des.* 9, 55–63. doi:10.1007/s10999-012-9205-7

Agius, S. L., Magniez, K. J. C., and Fox, B. L. (2013). Cure behaviour and void development within rapidly cured out-of-autoclave composites. *Compos. Part B Eng.* 47, 230–237. doi:10.1016/j.compositesb.2012.11.020

Carbas, R. J. C., Marques, E. A. S., Da Silva, L. F. M., and Lopes, A. M. (2014). Effect of cure temperature on the glass transition temperature and mechanical properties of epoxy adhesives. *J. Adhesion* 90, 104–119. doi:10.1080/00218464.2013.779559

Centea, T., Grunenfelder, L. K., and Nutt, S. R. (2015). A review of out-of-autoclave prepregs – material properties, process phenomena, and manufacturing considerations. *Compos. Part A Appl. Sci. Manuf.* 70, 132–154. doi:10.1016/j.compositesa.2014.09.029

Chen, W., Li, P., Yu, Y., and Yang, X. (2008). Curing kinetics study of an epoxy resin system for T800 carbon fiber filament wound composites by dynamic and isothermal DSC. *J. Appl. Polym. Sci.* 107, 1493–1499. doi:10.1002/app.26861

Costa, M. L., Almeida, S. F. M. D., and Rezende, M. C. (2001). The influence of porosity on the interlaminar shear strength of carbon/epoxy and carbon/bismaleimide fabric laminates. *Compos. Sci. Technol.* 61, 2101–2108. doi:10.1016/s0266-3538(01)00157-9

Cruz-Cruz, I., Ramírez-Herrera, C. A., Martínez-Romero, O., Castillo-Márquez, S. A., Jiménez-Cedeño, I. H., Olvera-Trejo, D., et al. (2022). Influence of epoxy resin curing kinetics on the mechanical properties of carbon fiber composites. *Polymers* 14, 1100. doi:10.3390/polym14061100

Ding, J., Peng, W., Luoac, T., and Yu, H. (2017). Study on the curing reaction kinetics of a novel epoxy system. *RSC Adv.* 7, 6981–6987. doi:10.1039/c6ra25120j

Dong, A., Zhao, Y., Zhao, X., and Yu, Q. (2018). Cure cycle optimization of rapidly cured out-of-autoclave composites. *Materials* 11, 421. doi:10.3390/ma11030421

Ferdosiana, F., Yuan, Z., Andersonb, M., and Xua, C. (2015). Sustainable lignin-based epoxy resins cured with aromatic and aliphatic amine curing agents: Curing kinetics and thermal properties. *Thermochim. Acta* 618, 48–55. doi:10.1016/j.tca.2015.09.012

Hernández, S., Sket, F., Molina-Aldareguı´A, J. M., González, C., and Llorca, J. (2011). Effect of curing cycle on void distribution and interlaminar shear strength in polymer-matrix composites. *Compos. Sci. Technol.* 71, 1331–1341. doi:10.1016/j.compscitech.2011.05.002

Hou, T.-H., Miller, S. G., Williams, T. S., and Sutter, J. K. (2013). Out-of-autoclave processing and properties of bismaleimide composites. *J. Reinf. Plastics Compos.* 33, 137–149. doi:10.1177/0731684413503050

Hubert, P., and Poursartip, A. (1998). A review of flow and compaction modelling relevant to thermoset matrix laminate processing. *J. Reinf. Plastics Compos.* 17, 286–318. doi:10.1177/073168449801700402

Kim, D., Centea, T., and Nutt, S. R. (2014). *In-situ* cure monitoring of an out-of-autoclave prepreg: Effects of out-time on viscosity, gelation and vitrification. *Compos. Sci. Technol.* 102, 132–138. doi:10.1016/j.compscitech.2014.07.027

Leena, K., Soumyamol, P. B., Monisha, B. A. B. Y., Suraj, S., Rajeev, R., and Mohan, D. S. (2017). Non-isothermal cure and decomposition kinetics of epoxy–imidazole systems. *J. Therm. Anal. Calorim.* 130, 1053–1061. doi:10.1007/s10973-017-6410-5

Li, Y., Zhang, Z., Li, M., and Gu, Y. (2007). Numerical simulation of flow and compaction during the cure of laminated composites. *J. Reinf. Plastics Compos.* 26, 251–268. doi:10.1177/0731684407070046

Lionetto, F., Buccoliero, G., Pappadà, S., and Maffezzoli, A. (2017). Resin pressure evolution during autoclave curing of epoxy matrix composites. *Polym. Eng. Sci.* 57, 631–637. doi:10.1002/pen.24568

Liu, D., Ji, P. Y., Xiao, L. H., and Ting, T. (2020). Fabrication and characterization of a modified conjugated molecule-based moderate-temperature curing epoxy resin system. *Front. Mat.* 7, 577962. doi:10.3389/fmats.2020.577962

Liu, Z., Zeng, J., Xiao, J., Jiang, D., and Peng, C. (2011). Rheological behaviors and processing windows of low viscosity epoxy resin for VIMP. *J. Wuhan. Univ. Technol. -Mat. Sci. Ed.* 26, 931–934. doi:10.1007/s11595-011-0339-5

Martínez-Miranda, M. R., García-Martínez, V., and Gude, M. R. (2019). Gel point determination of a thermoset prepreg by means of rheology. *Polym. Test.* 78, 105950. doi:10.1016/j.polymertesting.2019.105950

Marycheva, A. N. (2014). Investigation of the influence of rheological properties of binders to the heat resistance of polymeric composite materials. *nv.*, 81–85. doi:10.17117/nv.2014.02.081

Meola, C. (2020). Nondestructive testing in composite materials. *Appl. Sci. (Basel).* 10, 5123. doi:10.3390/app10155123

Mooney, P. (1991). Recent developments in the competition between advanced polymer matrix composites and metals in the manufacture of. *Mater. Process. Rep.* 6, 4–6. doi:10.1080/08871949.1991.11752446

Moreau, X. C. A. J. D. A. G., Delozanne, J., and Moreau, G. (2021). New advances in the kinetic modeling of thermal oxidation of epoxy-diamine networks. *Front. Mat.* 8. doi:10.3389/fmats.2021.720455

Mortimer, S., Ryan, A. J., and Stanford, J. L. (2001). Rheological behavior and gel-point determination for a model lewis acid-initiated chain growth epoxy resin. *Macromolecules* 34, 2973–2980. doi:10.1021/ma001835x

Orifici, A. C., Thomson, R. S., Degenhardt, R., Kling, A., Rohwer, K., and Bayandor, J. (2008). Degradation investigation in a postbuckling composite stiffened fuselage panel. *Compos. Struct.* 82, 217–224. doi:10.1016/j.compstruct.2007.01.012

Panettieri, E., Fanteria, D., Montemurro, M., and Froustey, C. (2016). Low-velocity impact tests on carbon/epoxy composite laminates: A benchmark study. *Compos. Part B Eng.* 107, 9–21. doi:10.1016/j.compositesb.2016.09.057

Pang, W., Shi, R., Wang, J., Ping, Q., Sheng, X., Li, N., et al. (2021). Research on resin used for impregnating polyimide fiber paper-based composite materials. *Materials* 14, 4909. doi:10.3390/ma14174909

Pethrick, R. A., and Hayward, D. (2002). Real time dielectric relaxation studies of dynamic polymeric systems. *Prog. Polym. Sci.* 27, 1983–2017. doi:10.1016/s0079-6700(02)00027-8

Schechter, S. G. K., Centea, T., and Nutt, S. R. (2018). Polymer film dewetting for fabrication of out-of-autoclave prepreg with high through-thickness permeability. *Compos. Part A Appl. Sci. Manuf.* 114, 86–96. doi:10.1016/j.compositesa.2018.08.002

Skordos, A. A., and Partridge, I. K. (2004). Determination of the degree of cure under dynamic and isothermal curing conditions with electrical impedance spectroscopy. *J. Polym. Sci. B. Polym. Phys.* 42, 146–154. doi:10.1002/polb.10676

Takagaki, K., Hisada, S., Minakuchi, S., and Takeda, N. (2016). Process improvement for out-of-autoclave prepreg curing supported by *in-situ* strain monitoring. *J. Compos. Mat.* 51, 1225–1237. doi:10.1177/0021998316672001

Torres, J. J., Simmons, M., Sket, F., and González, C. (2018). An analysis of void formation mechanisms in out-of-autoclave prepregs by means of X-ray computed tomography. *Compos. Part A Appl. Sci. Manuf.* 117, 230–242. doi:10.1016/j.compositesa.2018.11.010

Uthemann, C., Jacobsen, L., and Gries, T. (2017). Cost efficiency through load-optimised and semi-impregnated prepregs. *Lightweight Des. Worldw.* 10, 18–21. doi:10.1007/s41777-017-0052-y

Wang, R.-M., Zheng, S.-R., and Zheng, Y.-P. (2011). Fabrication of the half-finished products for polymer composites. *Polym. Matrix Compos. Technol.* 2011, 213–548. doi:10.1533/9780857092229.2.213

Wang, X, Jia, P., and Wang, B. (2022). Progressive failure model of high strength glass fiber composite structure in hygrothermal environment. *Compos. Struct.* 280, 114932. doi:10.1016/j.compstruct.2021.114932

Zhou, Z., Jiang, B., Chen, X., Jiang, F., and Jian, Y. (2014). Rheological behavior and process prediction of low viscosity epoxy resin for RTM. *J. Wuhan. Univ. Technol002E -Mat. Sci. Ed.* 29, 1078–1082. doi:10.1007/s11595-014-1046-9

Zhu, L., Wang, Z., Rahman, M. B., Shen, W., and Zhu, C. (2021). The curing kinetics of E-glass fiber/epoxy resin prepreg and the bending properties of its products. *Materials* 14, 4673. doi:10.3390/ma14164673